Mon. Not. R. Astron. Soc. **000**, 000–000 (0000) Printed 2 February 2008 (MN LATEX style file v1.4)

XMM-Newton Surveys of the CFRS Fields - I: The Sub-mm/X-ray relation ⋆

Timothy J. Waskett[1], Stephen A. Eales[1], Walter K. Gear[1], Elizabeth M. Puchnarewicz[2], Simon Lilly[3], Hector Flores[4], Tracy Webb[5], David Clements[6], Jason A. Stevens[7], Trinh X. Thuan[8]

[1] *Department of Physics and Astronomy, University of Wales Cardiff, PO Box 913, Cardiff, CF24 3YB, UK*
[2] *Mullard Space Science Laboratory, University College London, UK*
[3] *Herzberg Institute for Astrophysics, Dominion Astronomical Observatory, National Research Council, Canada*
[4] *Observatoire de Paris, Section de Meudon, DAEC, 92195 Meudon Principal Cedex, France*
[5] *Department of Astronomy and Astrophysics, University of Toronto, Canada*
[6] *Physics Department, Blackett Laboratory, Imperial College, London, UK*
[7] *UK Astronomical Technology Centre, Royal Observatory, Blackford Hill, Edinburgh EH9 3HJ*
[8] *Department of Astronomy, University of Virginia, P.O. Box 3818, Charlottesville, VA 22903*

arXiv:astro-ph/0301610v1 30 Jan 2003

2 February 2008

ABSTRACT

First results from *XMM-Newton* observations of the Canada France Redshift Survey (CFRS) 3hr, 10hr and 14hr fields are presented. Limited regions of two of the XMM surveys (3 and 14hr) are compared to the Canada UK Deep sub-mm Surveys (CUDSS) undertaken with SCUBA. None of the 27 SCUBA sources in the 3hr field are detected by XMM, while one of the 23 SCUBA sources in the 14hr field is found to coincide with an X-ray source. The SCUBA population as a whole is not significantly detected in either the $0.5-2$ keV or the $2-10$ keV X-ray bands, even after coadding the X-ray flux at the SCUBA positions, in both fields. The 18 X-ray sources within the CUDSS 3hr map yield a mean sub-mm flux of 0.48 ± 0.27 mJy after coadding the sub-mm flux at the X-ray positions. Using this result we place an upper limit on the contribution of AGN to the sub-mm background at 850 μm of ~ 7 *per cent*. Conversely we estimate the contribution of sub-mm sources to the $0.5-2$ keV X-ray background to be < 16.5 *per cent*. These results strongly support the conclusion that the two backgrounds are caused by different processes, in the one case nucleosynthesis in stars, in the other accretion onto black-holes. We conclude that it is possible for SCUBA sources in general to contain AGN, as long as they are Compton-thick and are at $z > 2.3$. The ratio of the X-ray to sub-mm flux for the X-ray sources however, implies that even when a galaxy does contain an AGN, most of the energy heating the dust is from young stars and not from the active nucleus.

Key words: galaxies:active – galaxies:starburst – diffuse radiation

1 INTRODUCTION

Recent advances in sub-mm astronomy have allowed rapid progress in our understanding of the early Universe. This region of the electromagnetic spectrum has largely been opened up by the powerful instrumentation that has become available within the last decade. One of the key instruments in this field has been the sub-mm Common User Bolometer Array (SCUBA), operating primarily at 850 μm, at the Naysmith focus of the 15m James Clerk Maxwell Telescope (JCMT) on Mauna Kea in Hawaii. Since its commission, deep surveys with SCUBA (Smail, Ivison & Blain 1997; Hughes et al. 1998; Barger et al. 1998; Eales et al. 1999) have resolved a significant fraction of the recently discovered far-IR and sub-mm background (Puget et al. 1996; Fixsen et al. 1998; Hauser et al. 1998), also called the Cosmic IR Background (CIRB). The importance of this becomes clear when one considers that the total integrated energy observed in the CIRB is comparable to the total integrated energy associated with the optical-UV background. Dust is very im-

⋆ Based on observations obtained with *XMM-Newton*, an ESA science mission with instruments and contributions directly funded by ESA Member States and NASA

© 0000 RAS

portant in the interstellar medium as it absorbs optical-UV photons and re-radiates far-IR photons, thus affecting our view of the Universe. Since this is the mechanism that produces most of the CIRB, it is possible that half of the light ever emitted by stars has been reprocessed by dust. However, there is one other mechanism that could contribute to this background light and that is the absorption, by dust, of the radiation from Active Galactic Nuclei (AGN).

In the standard model of AGN the central black hole is fed by an accretion disc (eg. Antonucci 1993). Around this disc lies a torus of heavily obscuring material containing large amounts of dust (eg. Nenkova, Ivezić & Elitzur 2002). If viewed close to the axis the AGN may be visible directly, in which case a Quasar or a Type-I Seyfert Galaxy is observed, with characteristic broad spectroscopic lines. Evidence for the obscuring torus comes from observations of Type-II Seyfert Galaxies, which in this model are seen edge-on. type-I emission, which would indicate the presence of an AGN, can only be indirectly observed by reflection off material above and below the torus. Direct evidence for the torus itself comes from its interaction with the nuclear radiation. The AGN heats up the torus which produces primarily mid-IR emission, but there will also be sub-mm emission from the dust. The process is much the same as in starlight re-processing, but here it is mainly UV and X-ray photons that are absorbed, and the dust tends to be hotter. Models suggest that between 5 and 30 *per cent* of the CIRB might be produced in this way (Gunn & Shanks 1999; Almaini, Lawrence & Boyle 1999). Franceschini, Braito & Fadda (2002) argue for the revision of this standard model, and suggest that Type-I and Type-II AGN are different populations that follow unrelated evolutionary paths, in particular at high redshifts. As deeper and more extensive X-ray/mid-IR surveys are collated this possibility will be tested more thoroughly, and a more complete picture of AGN may emerge.

The Cosmic X-ray Background (XRB) on the other hand contains much less energy than the optical or IR backgrounds ($\sim 1/100\ th$ depending on the definition). With the advent of powerful new X-ray telescopes such as *Chandra* and *XMM-Newton*, it has become possible to resolve most of this background radiation into discrete sources (eg. Rosati et al. 2002; Hasinger et al. 2001). The simplest form of the XRB is a power law defined as,

$$N = KE^{-\Gamma}$$

where N is the number of photons per second per cm^2 per keV, K is a normalisation constant and Γ is the photon index. This reaches a peak in energy density at $\sim 30\ keV$, and below this it has a very hard spectrum with a photon index $\Gamma = 1.4$. The most completely resolved part is the soft XRB ($0.5 - 2\ keV$), which is dominated by unobscured AGN and QSOs but these sources have much steeper (i.e. $\Gamma > 1.4$) spectral shapes than the XRB and cannot explain the spectrum at harder energies. Therefore, a population of more heavily obscured AGN, with flatter spectral shapes, is likely to be involved in the production of the hard XRB. The resolution of the XRB is less complete at these higher energies, although *XMM-Newton* with its sensitivity up to energies of $10\ keV$, is making a major contribution here. The deepest X-ray surveys with *Chandra* and *XMM-Newton* are beginning to reveal a population of highly obscured AGN (eg. Hasinger et al. 2001). An obvious possibility is that these highly obscured AGN, responsible for the hard XRB, are also producing the CIRB.

The most direct way of testing this, of course, is to make X-ray observations of the sources revealed by the deep SCUBA surveys. The studies which have so far been carried out (Almaini et al. 2001; Fabian et al. 2000; Hornschemeier et al. 2000) suggest that SCUBA sources are not generally X-ray sources.

In this paper we report our first results from *XMM-Newton* X-ray surveys of the Canada France Redshift Survey fields (Lilly et al. 1995). The 3hr and 14hr fields coincide with large and deep SCUBA surveys (Webb et al. 2002 & Eales et al. 2000), and so we report on the sub-mm/X-ray relation. The 10hr field coincides with a much smaller SCUBA survey, so it is not analysed in this paper. It is mentioned here for completeness, with full multi-wavelength analysis of all three fields reserved for a future paper.

Assumed cosmology: $H_0 = 75\ km\ s^{-1}\ Mpc^{-1}$, $\Omega_m = 1$ and $\Omega_\Lambda = 0$.

2 X-RAY DATA REDUCTION

The data for the 3hr field were taken on 17th February 2001 by *XMM-Newton* over a period of 51.5 ks, using the thin filters and in imaging mode. All three primary instruments gathered data (MOS 1, MOS 2 & PN) as well as the optical monitor (OM) telescope. This field is centred on R.A. 03:02:38.60 Dec. +00:07:40.0.

The 10hr field was similarly surveyed by XMM for 50.8 ks, using the thin filter for the PN instrument and the medium filter for the two MOS instruments. This field is centred on R.A 10:00:40.4 Dec. +25:14:20.0.

The 14hr field data was obtained from the public archive after the proprietary period had expired, to complete our coverage of available XMM data for the CFRS fields. This data was first presented in Miyaji & Griffiths (2001). Of the several available exposures of this field, one was selected that most closely matched the exposures of the other two fields. The exposure was taken over 56.1 ks, using thin filters, and is centred on R.A. 14:17:12.0 Dec. +52:24:00.0. We do not discuss the Optical Monitor data here, for any of the above surveys.

The *XMM-Newton* raw data were processed using version 5.3 of an ensemble of tasks collectively titled Science Analysis System (SAS). These tasks allow re-running of basic pipeline processes as well as further data reduction tasks. Initial pipeline processing of the EPIC instruments is achieved through the running of the tasks 'emproc' for the two MOS instruments and 'epproc' for the PN instrument. This produces the basic calibrated photon event files (recording the time, position and energy of each photon) which are used in all further processing. These tasks also remove hot and flickering pixels and columns.

Filtering of the event files is essential to obtain usable data, and so this is the next step. Non X-ray associated events such as cosmic rays create patterns on the detectors that look different from the impacting of X-rays. These events are flagged and filtered out. On the other hand soft protons, produced by the sun and projected towards Earth in solar flares, produce patterns that look identical to X-

rays. Therefore these need to be filtered out by generating a rate curve displaying the count rate for an instrument as a function of time. It is clear from this rate curve when flaring events occur during the observation, because of the vast increase in the count rate, and so the affected time intervals can be removed from the data completely. For the data in this work flaring events cause a loss of ~ 20 *per cent* of the total observing time in the 3hr field and ~ 10 *per cent* for the 10hr field. The 14hr field was less affected by flares and so only ~ 2 *per cent* of data had to be removed.

Specific energy channels can also be selected, enabling images in different energy bands to be produced. Two bands are used in this work, a soft band and a hard band, corresponding to $0.5-2$ keV and $2-10$ keV respectively. The low end 0.5 keV cutoff ensures that X-ray emission from the Galaxy, which is greatest below this level, is kept to a minimum. Attenuation of soft X-rays by Galactic HI is also more pronounced at energies lower than this cutoff and so this too is avoided. The high energy limit of 10 keV is set by the instrument response, which decreases rapidly at higher energies, more so for the MOS instruments than the PN instrument.

The remaining noise is primarily due to the quiescent internal instrument background caused by high energy particles interacting with the structure surrounding the detectors. There is also detector noise but this is negligible and only becomes important at energies below ~ 0.5 keV. Due to the small number of photons involved in X-ray observations additional noise is introduced by the poissonian statistics, and ultimately this is the dominant source of error in the measurements.

Once filtering is complete images are produced for each instrument in the two energy bands. Free from bad pixels, flaring events and non X-ray associated events the images can then be passed through the source detection procedure. This is a multi-stage process performed on the combined bands for all three EPIC instruments simultaneously, so that the maximum amount of information is used in determining the source parameters. The process is summarised here.

First, a sliding box source detection algorithm is run on the images which flags any region that exceeds a minimum likelihood limit of 10 (equivalent to about 4 σ) as a source. The likelihood limit L is defined such that $L = -\ln P$, where P is the probability of finding an excess above the background which is not due to a source. The source list produced by this first pass is used to create a "cheese" map whereby all objects in the list are removed from the image which is then interpolated using a spline to create a smooth background ready for the second pass of the sliding box procedure. The combined list from both passes is then fed into a maximum likelihood (ML) algorithm which compares each object with a point spread function (PSF) model to determine a confidence level for it being a source. All objects below a threshold (higher than for the sliding box) are rejected leaving the final source list. This method of source detection is discussed in more detail in Valtchanov et al (2001), and is compared against other methods for detecting sources in *XMM-Newton* images. In this work a ML limit of 15 is used, to minimise the number of false detections.

In total 451 sources are detected in the three exposures, in one or more instrument or band. These are divided as follows: 146 in the 3hr field, 151 in the 10hr field and 154 in the 14hr field. Full discussion of the X-ray sources, together with catalogues, are reserved for a future paper. For this work only the areas observed in the Canada-UK Submillimeter Survey (CUDSS) are considered.

Using two X-ray bands it is possible to define a quantity called the hardness ratio, which gives an indication as to the basic spectrum of a source. For this work it is defined as:

$$HR = \frac{N(H) - N(S)}{N(H) + N(S)}$$

where $N(H)$ and $N(S)$ are the counts observed for a source in the hard and soft bands respectively, after correction for vignetting. Higher values indicate a harder spectrum.

The minimum detected flux for these surveys is $\sim 0.2 \times 10^{-15}$ $erg\ cm^{-2}\ s^{-1}$ in the soft band, $\sim 1 \times 10^{-15}$ $erg\ cm^{-2}\ s^{-1}$ in the hard band and $\sim 1 \times 10^{-15}$ $erg\ cm^{-2}\ s^{-1}$ in the full $(0.5-10\ keV)$ band. However, the cumulative source counts begin to deviate from the expected power law at fluxes of about 0.6, 3 and 3×10^{-15} $erg\ cm^{-2}\ s^{-1}$ in the respective bands, thus we estimate that the surveys are 100 *per cent* complete at these fluxes.

The astrometry for the source lists are compared to known QSOs in each field and corrected as appropriate. The IDing process, to be discussed more fully in a future paper, was carried out on the corrected source positions. As a second additional check for systematic errors in the X-ray astrometry, the mean offset between the X-ray sources and the IDs was calculated. The residuals after correction revealed no further systematic offsets.

XMM has a typical astrometric accuracy of $2''$ for sources near the pointing axis, but this deteriorates gradually for progressively larger off-axis angles. At the depth of these surveys XMM does not suffer from source confusion, which would become important for exposure times of $\sim 150-200$ ks. The principle limit in this study is the performance of SCUBA which has a beam size over twice that of XMM. In comparison *Chandra* has significantly better resolution at $0.5''$ astrometric accuracy, and has a lower detector background than XMM, but it is less sensitive (particularly at energies > 8 keV) and has a mirror effective area less than 1/5th that of XMM.

The composite images shown in this work are a result of merging images from the PN and two MOS instruments together using the SAS task 'emosaic'. This task is only used in this instance to produce a clear image, and is not used for further analysis of the data, except for the statistical tests described in section 3.2. See figs. 1 and 2.

The majority of the work presented in this paper concentrates on the 3hr XMM field and the corresponding CUDSS region which lies in the centre of the XMM FoV. The 14hr field is also part of CUDSS but the survey region lies towards the edge of the XMM FoV, and the X-ray data are therefore less reliable.

3 SCUBA SOURCES

There are 27 sources detected at 850 μm in the 3hr CUDSS field, spanning a region of approximately $9' \times 6.4'$ (Webb et al. 2002). This lies in the central part of the *XMM-Newton* FoV which is roughly circular with a diameter of $\sim 30'$.

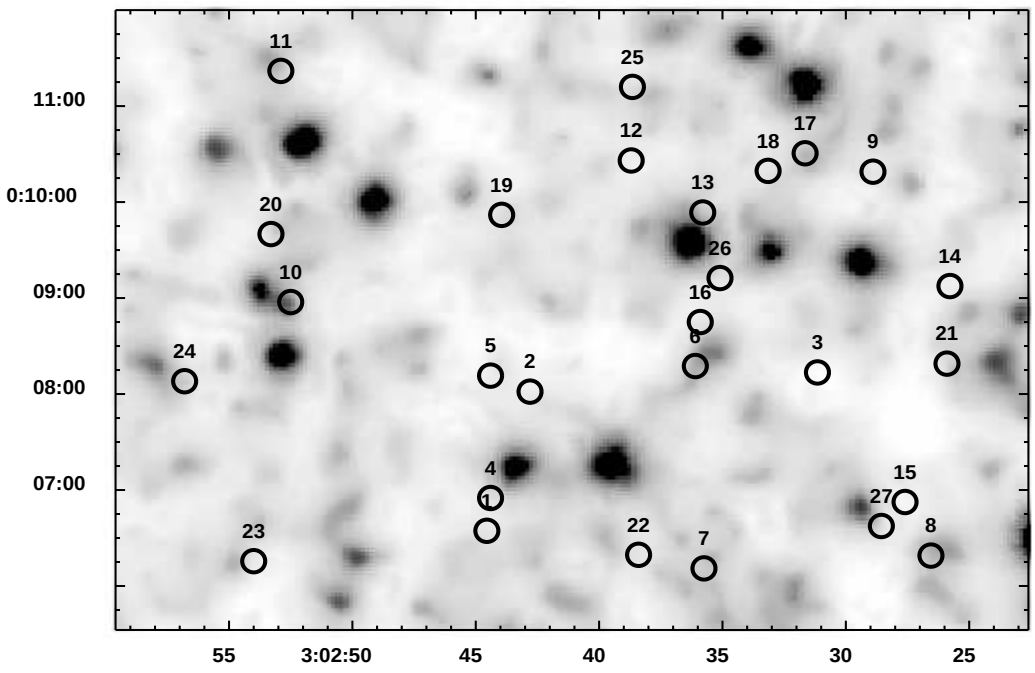

Figure 1. The central part of the 3hr XMM survey showing the 3hr CUDSS region in the soft X-ray band, for clarity. Overlayed are 14″ diameter circles at the positions of the SCUBA sources. Numbers and positions are from Webb et al. (2002).

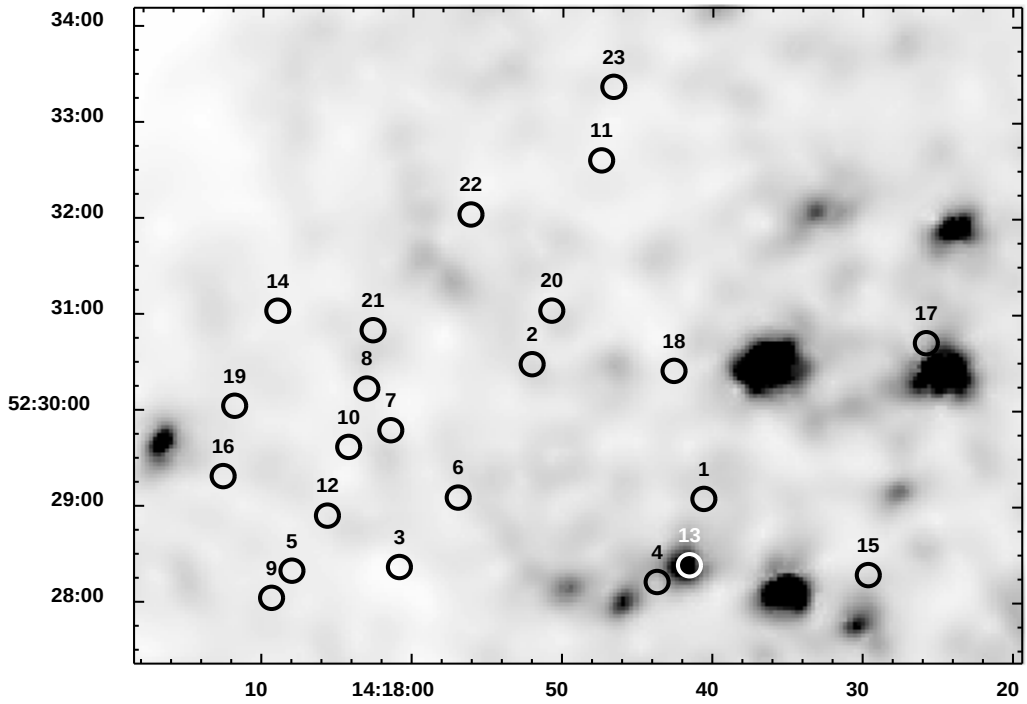

Figure 2. As fig 1 but for North-East part of the 14hr XMM survey showing the 14hr CUDSS region. Numbers and positions are from Eales et al. (2000) and Webb et al. (in preparation). The pattern of X-ray sources in this plot is mainly due to natural variations in number density across the sky, and the domination of two QSOs near the right edge, although the far top left may suffer slightly from the declining sensitivity of XMM towards the edge of its FoV.

The 14hr CUDSS field is approximately $7.7' \times 6.4'$ (Eales et al. 2000) and is centred about $8.5'$ North-East of the XMM pointing axis. This map contains 23 sources.

3.1 X-ray properties of the SCUBA sources

The first thing to do when comparing sources in the same area but different parts of the spectrum is to see if any of them match up. An inexact match-up does not necessarily mean that two objects are unassociated, because of the error in the positional accuracy of both sets of objects, caused by the finite resolution of the instruments involved. For SCUBA the FWHM of the 850 μm beam is $\sim 14''$, whereas for XMM the on-axis FWHM is $\sim 6''$, which increases with larger off-axis angles. For the purposes of this work the XMM PSF can be considered constant, and equal to $6''$, across the area containing the 3hr SCUBA sources, as this is a small fraction of the total XMM FoV. As for the 14hr field, the off-axis angle of the CUDSS map means that the XMM PSF is not so well behaved, and further analysis less reliable. However, as an approximation the FWHM has a median value of $\sim 9''$ across the 14hr CUDSS map.

3.1.1 The 3hr Field

Of the 27 SCUBA sources in the 3hr field only one (CUDSS 3.10) is possibly associated with a region of faint X-ray emission. The flux of this region is below the flux limit of the survey, but it appears as a faint patch in the smoothed image, fig. 1. This region was picked up by an earlier version of the detection software at the thresholds used, however after re-analysis with the updated software, which has better calibration, this source is no longer detected using the same thresholds. An additional degree of uncertainty exists for this region, because it lies on a boundary between two PN CCD chips. Source detection near chip edges is less precise than in the centre of chips, so this possible associations should be regarded with extreme caution.

Given the position of the SCUBA sources the probability that there is a chance coincidence with an unrelated X-ray source within a distance r is given by poissonian statistics as:

$$P = 1 - exp(-\pi n r^2)$$

where n is the surface density of X-ray sources.

CUDSS 3.10 lies $\sim 3.6''$ from the centre of the region of faint X-ray emission (given by the detection with the earlier version of SAS). The surface density of X-ray sources at the flux limit of this survey is $n = (5.7 \pm 0.5) \times 10^{-5}$ per square arc second, thus for this source, which is below the flux limit, $P > 0.0023$. A deeper exposure of this region would determine if this X-ray region is actually a source, and thus a significant association, or just noise.

3.1.2 The 14hr Field

Figure 2 shows the CUDSS 14hr map as viewed in soft X-rays with the SCUBA sources overlayed. CUDSS 14.13 is clearly near a significant X-ray source, and this is indeed detected by the XMM source detection software. This X-ray source has a soft band flux of $(6.7 \pm 0.51) \times 10^{-15}$ $erg\ cm^{-2}\ s^{-1}$ and a hard band flux of $(2.2 \pm 0.25) \times 10^{-14}$ $erg\ cm^{-2}\ s^{-1}$, assuming a power law photon index of 1.4. The positional offset is $4.8''$, and the surface density of X-ray sources brighter than the flux of this source is $n = (4.5 \pm 0.4) \times 10^{-5}$ per square arc sec. This leads to $P = (3.3 \pm 0.2) \times 10^{-3}$ for this coincidence.

Webb et al. (in preparation) discuss this SCUBA source to some extent. It is identified with the optical source CFRS14.1157, which is $1.2''$ from the position of our X-ray detection. This source is also detected in the radio (Eales et al. 2000) and by ISO making it an interesting source. It also has a spectroscopically measured redshift of $z = 1.15$ (Hammer et al. 1995). The optical/NIR colours are very red, $(I-K)_{AB} = 2.6$, consistent with an irregular or spiral galaxy with high extinction, and the X-ray hardness ratio is quite high (~ -0.3) implying that this is a fairly heavily obscured object. HST imaging of this object shows a disturbed morphology (Webb et al. in preparation), suggesting the X-ray activity may be related to a possible interaction.

By taking the measured redshift for this source, and the X-ray flux in the two bands, it is possible to estimate the column density of neutral hydrogen responsible for the obscuration of the X-rays. If we assume an intrinsic photon index of $\Gamma = 2.0$ (Hasinger et al. 2001) then a column density of $N_H = 3.0 \times 10^{22}\ cm^{-2}$ produces the correct X-ray fluxes.

It is interesting to ask at this point whether, assuming an AGN is responsible for the X-ray emission, it can also be responsible for the sub-mm flux measured by SCUBA (through the heating of dust). By assuming that 3 *per cent* of the bolometric luminosity of an unobscured AGN (optical through to X-ray) is emitted in the $0.5 - 2\ keV$ band (Page et al. 2001), and correcting for the intrinsic absorption, the AGN has a total luminosity of $(2.6 \pm 0.2) \times 10^{11} L_\odot$.

The far-IR luminosity on the other hand is $(5.1 \pm 1.5) \times 10^{12} L_\odot$, assuming a single dust temperature of $40K$ and $\beta = 1.5$. This means that the AGN is 20 times less luminous and so cannot possibly power the far-IR luminosity on its own. The majority of the far-IR luminosity must therefore be powered by star-formation, and in-fact Webb et al. (in preparation) estimate a star-formation rate of 210 $M_\odot\ Yr^{-1}$ assuming that the far-IR luminosity is produced in this way. However, the far-IR luminosity is highly model dependent and can be much lower, for example a single temperature dust component of $< 20K$ gives a far-IR luminosity low enough to be equal to the AGN luminosity. Although this model is unlikely in light of the high inferred star formation rate which would result in at least some warm dust, and this would push up the luminosity greatly. For example, a two dust component model with 50 times as much cold dust ($15K$) as warm dust ($45K$) and $\beta = 2$ (e.g. Dunne & Eales 2001) has a far-IR luminosity of $(2.2 \pm 0.7) \times 10^{12} L_\odot$, making it 8 times as luminous as the AGN. Thus, the conclusion that this source is dominated by star-formation and not an AGN is hard to avoid.

Further evidence for the star-formation activity of AGN host galaxies can be found in the 8 mJy SCUBA survey fields (Ivison et al. 2002). The X-ray detected SCUBA sources in these fields (15 *per cent*) are consistent with obscured AGN, but the AGN bolometric luminosities are not sufficient to power the far-IR luminosities, unless the X-ray emission is attenuated by Compton thick ($N_H > 10^{24}\ cm^{-2}$)

material. If not, star-formation is likely to be responsible instead.

Page et al. (2001) draw a similar conclusion for high redshift X-ray selected sources that have a SCUBA detection. For their sample the AGN luminosity and far-IR luminosity are more closely matched, being at most a factor of 4 different in favour of the far-IR luminosity. The main differences in this case are that the AGN in their sample are at higher redshift ($z = 1.5 - 3$) and are more luminous ($L_{AGN} > 4.36 \times 10^{12} L_{\odot}$) than CUDSS 14.13. The HI column densities in their sample are similar to CUDSS 14.13.

Whereas Page et al. (2001) target X-ray sources with SCUBA, a reverse study whereby bright SCUBA sources are observed with the *Chandra* X-ray observatory was carried out by Bautz et al. (2000). They measure the AGN/far-IR luminosity for two bright, lensed sub-mm sources at high redshift and find that the AGN is responsible for the majority of the far-IR luminosity in one and $\sim$ 40 *per cent* in the other, implying that some other power source must be responsible for the deficits.

3.2 Statistical analysis

The fact that only one out of 50 SCUBA sources matches an X-ray source does not mean that the population as a whole is not significantly emitting X-rays. A simple way to test this is to coadd the X-ray counts associated with each SCUBA source and see if the average X-ray flux of the SCUBA sources is statistically significant. We refer to this as the coadding technique.

The CUDSS 3hr map is located in the centre of the XMM FoV which lies entirely in the central CCDs of the two MOS arrays. However, the PN array contains many chip boundaries in this region, and several SCUBA sources lie on or near one of these boundaries. Therefore, to avoid possible problems caused by inconsistencies between sources, the PN data is not used in the analysis.

Due to the 14hr CUDSS map being off-axis in the XMM survey we consider the 3hr field to be more useful and accurate for study. However, for consistency, the 14hr field is analysed in the same way as the 3hr map, but is considered separately because of the difficulty in combining the results from the two regions in any sensible way. The following description relates to the 3hr field, with differences for the 14hr field noted where relevant.

The XMM optics spread out photons from a point source into several pixels in the images (the PSF). Although the pixel at the co-ordinates of the source should contain the peak of the emission, neighbouring pixels also contain information from the source. This effect is important for faint X-ray sources in particular because in some cases there may be no actual photon counts in the pixel corresponding to position of the source. Therefore, for analysis of the SCUBA sources in the X-ray images, the information from the whole PSF of XMM needs to be recovered and incorporated into the central pixel.

Images were accumulated in each band for the two MOS instruments and superimposed, as described at the end of section 2. They were then convolved with a 2D Gaussian of $FWHM = 6''$, the FWHM of the on-axis XMM beam ($9''$ for the 14hr field to reflect the larger, off-axis, PSF). This creates a map in which the signal in each pixel is the best possible estimate of the X-ray signal at that point. By smoothing the image with the XMM PSF (or a reasonable model for it in this case), the information in the central pixel contains all the information from the surrounding pixels, weighted according to how likely it is that the photons detected in those pixels came from the source. This technique for making the best estimate of the flux at a given point has been widely used in other wavebands (eg. Phillipps & Davies 1991; Eales et al. 2000), and is similar to the stacking technique used in the analysis of the *Chandra* Deep Fields (eg. Brandt et al. 2001).

The mean X-ray flux of the 27 SCUBA sources was determined for each energy band. To estimate the significance of the values a Monte-Carlo simulation was used. 30,000 random samples of SCUBA sources were produced at randomly selected positions within the CUDSS region, each with 27 sources. The mean X-ray flux for each sample was measured in the same way as for the real sample. The distribution of these means is shown in figs 3(a) and 3(b). The number of trial samples for which the mean equals or exceeds the observed sample mean is then calculated (See figures 4(a) and 4(b) for the 23 SCUBA sources in the 14hr field). A low number of trials exceeding the observation indicates a significantly important measurement.

Out of 30,000 random trials 2,010 equalled or exceeded the observation ($\sim$ 6.7 *per cent*) for the soft band and 25,800 ($\sim$ 86.0 *per cent*) for the hard band (see fig. 3(a) and 3(b)). A more restricted sample was also tested, in case some of the less secure SCUBA detections were in fact false. The 9 SCUBA sources with the highest flux produced $\sim$ 63.3 *per cent* and $\sim$ 62.4 *per cent* of trials that equalled or exceeded the observation, for the soft and hard bands respectively. Thus the SCUBA population is not detected, and is lost within the unresolved X-ray background. Converting the mean counts per SCUBA source into a mean flux gives a 99 *per cent* upper limit estimate of 1.25×10^{-16} *erg cm*$^{-2}$ *s*$^{-1}$ in the soft band and 6.62×10^{-16} *erg cm*$^{-2}$ *s*$^{-1}$ in the hard band, the true values falling below these limits 99 *per cent* of the time.

As an additional test, to take the accuracy of the SCUBA positions into account, we repeated this test by selecting the brightest X-ray pixel within a search radius of $4''$ of the given SCUBA position, instead of just taking the pixel value at that position. No significant difference was obtained, as the mean fluxes for both the randomly generated samples and the true samples increased by a similar number of X-ray counts, leading to similar significances and mean X-ray flux limits.

For the 14hr field 22.7 *per cent* and 7.4 *per cent* of trials equalled or exceeded the observation, in the soft and hard bands respectively (see figures 4(a) and 4(b)). The flux limits are less stringent than the 3hr field at 8.0×10^{-16} *erg cm*$^{-2}$ *s*$^{-1}$ in the soft band and 1.3×10^{-15} *erg cm*$^{-2}$ *s*$^{-1}$ in the hard band. This is likely to be a consequence of the 14hr CUDSS region being off-axis in the XMM survey. The vignetting of the telescope increases the flux limit towards the edge of the FoV because of the reduced effective exposure time compared to on-axis.

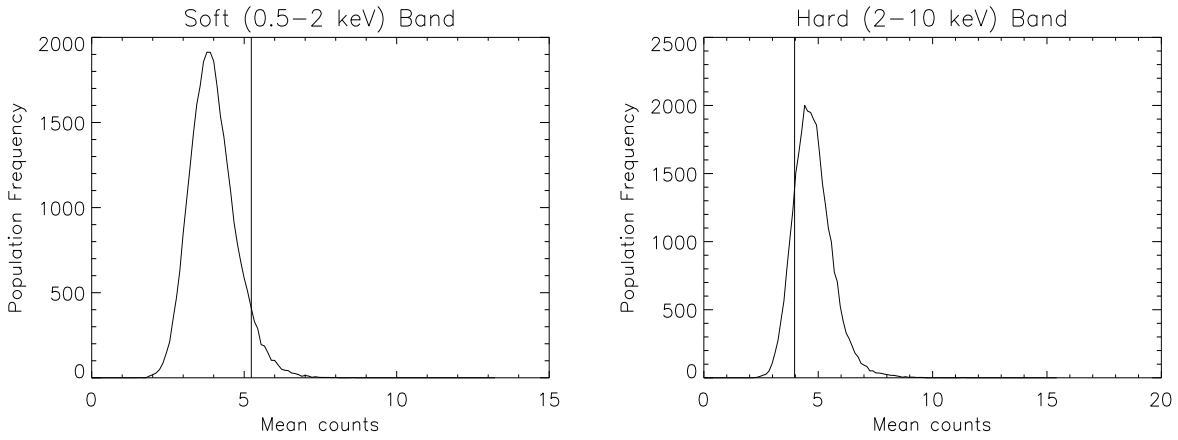

(a) (b)

Figure 3. Histograms showing the distribution of mean X-ray counts associated with each source for 30,000 artificial SCUBA samples in the 3hr field. Vertical lines represent the mean counts for the real SCUBA sources. See text for details.

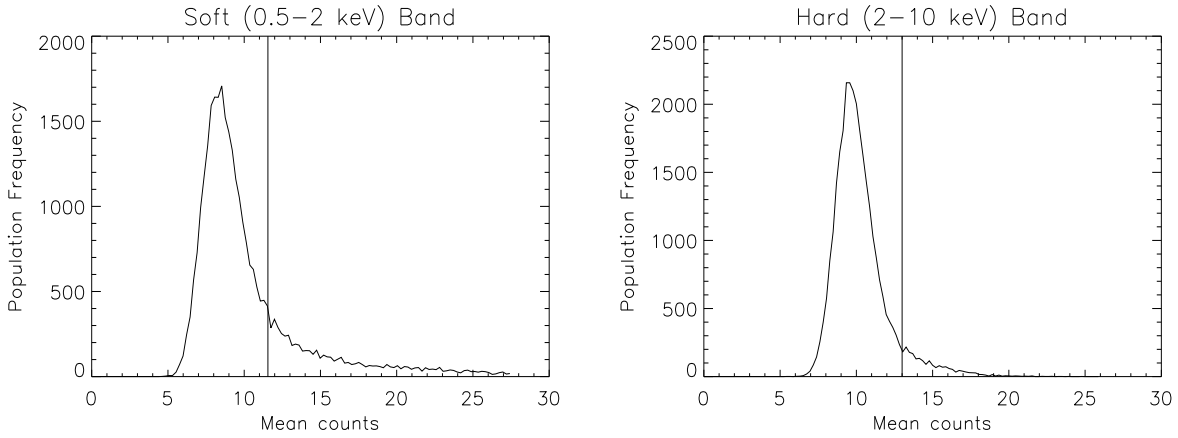

(a) (b)

Figure 4. As for figures 3(a) & 3(b) but for the 14hr field. This plot highlights the higher background in this field compared to the 3hr field, a feature of the survey itself rather than the poorer response of the instrument for large off-axis angles.

4 SUB-MM PROPERTIES OF X-RAY SOURCES

Taking the reverse approach, the sub-mm properties of the 18(16) X-ray sources within the 3hr(14hr) SCUBA maps can be determined. The SCUBA maps are heavily confused, not only from the positive sources but also the negative side lobes produced by the chopping procedure. Therefore, the SCUBA sources not associated with X-ray sources are removed from the map, including the side lobes. This reduces the confusion from known sources, in order to better test the low level emission in the map that is unresolved but may still be real, and associated with X-ray sources. After this procedure, the weighted mean 850 μm flux of the 3hr X-ray population is found to be $0.48 \pm 0.27\ mJy$. The 14hr field yields a mean 850 μm flux of $0.35 \pm 0.28\ mJy$. These are not significant detections, but are tentatively suggestive of dust emission.

These measurements are in contrast to the mean sub-mm flux of $1.69 \pm 0.27\ mJy$ obtained by Barger et al. (2001) for a sample of 136 X-ray sources selected in the $2 - 8\ keV$ band, detected in the Chandra Deep Field North. Although for a restricted sample of soft X-ray sources with $\Gamma > 1$ they find the mean sub-mm flux is much lower at $0.89 \pm 0.24\ mJy$, consistent with our 3 σ upper limits of 0.81 and 0.84 mJy for the two fields. This is also consistent with Almaini et al. (2001) who measure a noise weighted mean of $0.89 \pm 0.3\ mJy$ for their X-ray sources. It is perhaps not surprising that Barger et al. (2001) find many X-ray sources with hard spectra ($\Gamma < 1$), for which they measure a mean sub-mm

flux of 1.77 ± 0.21 mJy, since their sources are selected in a hard X-ray band. In contrast our sources are selected in the soft $0.5-2$ keV band as well as the hard $2-10$ keV band, and so there are many more sources with soft rather than hard spectra in our surveys. These soft sources dominate our sub-mm measurement which could partially explain our lower values.

An alternative explanation for the differing mean sub-mm measurements in different studies may come from the different methods used in calculating them. Not removing SCUBA sources that do not coincide with X-ray sources will result in higher residual sub-mm measurements than our method.

The mean soft X-ray flux for the X-ray sources in these two regions are $(1.8 \pm 0.1) \times 10^{-15}$ erg cm^{-2} s^{-1} for the 3hr CUDSS map and $(7.8 \pm 0.4) \times 10^{-15}$ erg cm^{-2} s^{-1} for the 14hr CUDSS map, measured in the soft band.

5 DISCUSSION

5.1 AGN Verses Star-formation

The lack of X-ray/SCUBA coincidences suggests three main possibilities. Either the X-ray survey is not deep enough to detect the AGN that may exist within the SCUBA sources; the AGN are obscured by Compton thick material, leading to very little nuclear radiation escaping unhindered ($N_H > 10^{24-25}$ cm^{-2}); or the SCUBA sources do not contain AGN.

Redshift information on the X-ray and SCUBA populations lends support to the separate population hypothesis. Recent deep X-ray surveys (Hasinger et al. 2001; Rosati et al. 2002; Mainieri et al. 2002) have determined the redshift distribution for large fractions of their sources. With a median redshift of < 1 these surveys differ from the AGN synthesis models (Gilli, Salvati & Hasinger 2001) which predict higher peak redshifts 0f 1.3-2. In contrast the deep SCUBA populations have been placed at much higher redshifts, typically $z \sim 2$ or greater (Ivison et al. 2002; Chapman et al. 2003), which would naturally explain the small overlap between the two observed populations.

Can we be sure that SCUBA sources are powered by star-formation and not by AGN? The latter is still a possibility, despite the low SCUBA/X-ray coincidence, as the AGN may be heavily obscured and as such not visible to this X-ray survey. NGC6240, for example, is known to be a starburst galaxy that also contains a heavily obscured AGN ($N_H > 2 \times 10^{24}$ cm^{-2}) (eg. Iwasawa & Comastri 1998; Lira et al. 2002). To compare the SCUBA sources to NGC6240 we use the SED for a 'high-reddening' starburst galaxy taken from Schmidt et al (1997). This fits the measurements for NGC6420 well (Lira et al. 2002). We use this SED as a basic template, modified for an X-ray photon index of 1.4 to approximate the broad characteristics of NGC6240 (Iwasawa & Comastri. 1998). We calculate the ratio between the soft X-ray flux and the 850 μm flux in the observed frame as a function of redshift, and this is plotted in fig. 5. We also plot the X-ray/sub-mm flux ratio for a typical Seyfert 2 galaxy with respect to redshift, using a template also taken from Schmidt et al. (1997).

The upper limit on the ratio of the mean X-ray to sub-mm flux for the SCUBA sample is consistent with the template for NGC6240 as long as the redshifts of the SCUBA sources are > 2.3. This is consistent with redshifts measured for many SCUBA sources (Ivison et al. 2002; Chapman et al. 2003), and so we conclude that in general it is still possible that most SCUBA sources may contain Compton thick AGN like NGC6240. Almaini et al. (2001) rule out the possibility that SCUBA sources are QSOs, unless they are Compton thick and at very high redshift, and show that they are consistent with a starburst template at $z > 2$. This is in general agreement with our results. The SCUBA sources with secure identifications and spectroscopic redshifts (Webb et al. 2002; Webb et al. in preparation) are also plotted for the two fields.

A similar plot for the X-ray sources is shown in fig. 5(b). Note that the 14hr field has a higher mean X-ray flux because this field is dominated by several bright X-ray sources (two are known QSOs, Schade et al. 1996).

In an alternative approach we can calculate the far-IR and AGN luminosities of the ensemble of X-ray sources in the 3hr CUDSS map, as we did with CUDSS 14.13 (section 3.1.2). We use the mean SCUBA flux measurement of 0.48 mJy at 850 μm, and assume a column density of 10^{22} cm^{-2} to be representative of the X-ray sources. For any reasonable far-IR SED the AGN luminosity, from optical through to X-ray, never exceeds the far-IR luminosity for redshifts below 2. If we require the entire sub-mm flux to be produced by the AGN then the X-ray sources must either be modestly absorbed at very high redshifts, or extremely highly absorbed and at lower redshifts. This shows that in general the bolometric luminosities of the X-ray sources in this field are probably dominated by star-formation in the same way as CUDSS 14.13 is. All of this, however, is highly speculative because of the highly model dependent nature of the far-IR luminosity calculation, and the marginal (not even 2 σ) sub-mm detection.

5.2 Extra-Galactic Background Radiation

The following analysis is based on the 3hr CUDSS region.

The upper limit on the average X-ray flux of the SCUBA sample also allows us to place an upper limit on the contribution the SCUBA population makes to the XRB. Our sub-mm sample constitutes about 20 *per cent* of the extra-galactic background at 850 μm, and so we scale our upper limit by a factor of 5 to calculate an upper limit on the contribution dust sources make to the XRB (assuming that the X-ray/sub-mm ratio is not dependent on sub-mm flux). The sample provides a maximum of 3.3 *per cent* of the XRB at $0.5-2$ keV, and so the population as a whole must contribute no more than 16.5 *per cent* in this band. In the hard band the SCUBA sample contributes an upper limit of 6.1 *per cent* to the XRB and so the population as a whole provides at most 30.7 *per cent*. It is clear that sub-mm sources do not dominate the X-Ray background at low energies, but it remains to be seen if their contribution to the peak of the XRB (~ 30 keV) is more significant.

Taking the opposite approach we can estimate the contribution of AGN to the 850 μm background. The simplest way is to convert our 3 σ upper limit sub-mm flux, as measured in section 4, of the detected X-ray sources into a smooth background by multiplying it by the number density of X-ray sources detected by our survey. Comparing this to the intensity of the CIRB at 850 μm gives an estimate of a

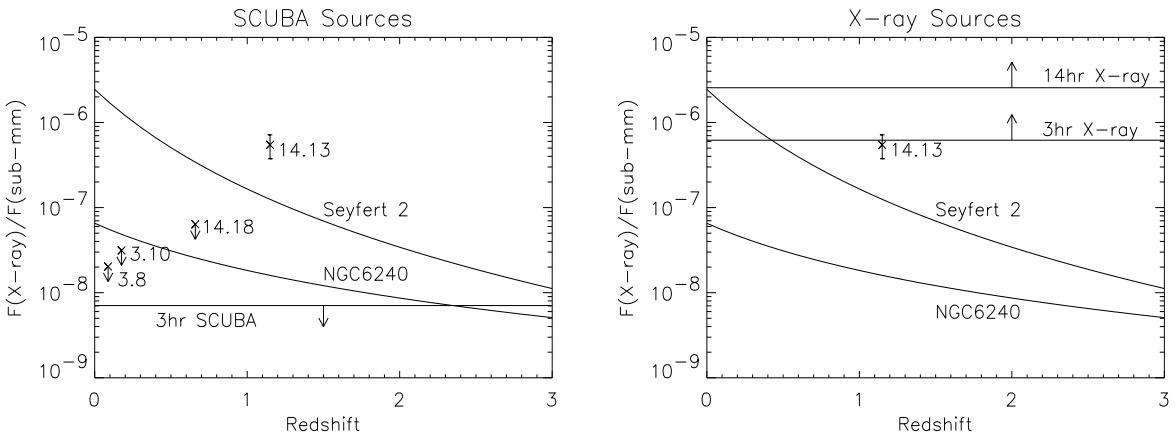

(a) (b)

Figure 5. X-ray to sub-mm flux ratios for the SCUBA sources (5(a)) and the X-ray sources (5(b)). Template SEDs of NGC6240 and a Seyfert 2 Galaxy are plotted for comparison. Horizontal lines represent the ratios of the measured mean fluxes for the 3hr sub-mm sample (5(a)), and the X-ray samples (5(b)). The only definite sub-mm/X-ray coincidence is plotted in 5(b), and is from Eales et al. (2000) with redshift from Webb et al (in preparation). The two 3hr SCUBA sources with secure IDs and spectroscopic redshifts (Webb et al. 2002) are plotted in 5(a) along with the only other 14hr SCUBA source with a secure ID and redshift (Webb et al. in preparation). The low z 3hr sources are not representative of the SCUBA population as a whole, which in general lie at higher z, and so do not necessarily have the same properties. Their optical counterparts both show merger morphology. Source labels are the CUDSS reference numbers.

2.3 *per cent* contribution from AGN. Assuming the 3hr field is a typical extra galactic region and that the X-ray sources are indeed AGN then this is a little low compared with theoretical models (eg. Almaini, Lawrence & Boyle 1999). Our X-ray survey, however, only resolves about 32 *per cent* of the X-ray background in the soft band. If we assume that the background we have not resolved has the same X-ray/sub-mm ratio as our X-ray sample, then 7.2 *per cent* of the sub-mm background is produced by the sources making up the X-ray background. This may be too low because the fainter X-ray sources may be more heavily obscured, and the results from the *Chandra* Deep Fields do suggest that the ratio decreases at lower X-ray flux (Barger et al. 2001). However, we have argued above that much of the sub-mm emission from X-ray sources is from dust heated by star-formation and not by AGN, and thus the estimate above is really an upper limit on the contribution of AGN to the sub-mm background. These two arguments work in opposite directions and may act to cancel each other out.

The contribution of the SCUBA sources to the X-ray background and of the X-ray sources to the sub-mm background strongly suggest the two backgrounds are disjoint, with the sub-mm background mostly produced by stellar nucleosynthesis and the X-ray background by accretion on to black-holes.

6 CONCLUDING REMARKS

This study adds weight to the growing body of evidence pointing to the fact that SCUBA sources may indeed contain active nuclei, but that their presence is secondary to starburst activity as a power source for their high far-IR luminosities. In some cases it is possible to view the active nucleus directly using current X-ray satellites, but there are still many SCUBA sources that show no evidence of X-ray emission. Higher and higher column densities of HI progressively wipe out X-ray emission up to higher energies, and as such are capable of putting AGN beyond detectability by current X-ray detectors sensitive only up to $\sim 10\ keV$. If this is the case for the majority of SCUBA sources then the scenario outlined above will need to be modified, as it is possible for the entire sub-mm luminosity of a SCUBA source to be powered by a very powerful but highly obscured AGN, with no need for a starburst. How common such highly obscured systems are is likely to remain uncertain until X-ray instruments become available with good spatial resolution and good sensitivity above $10\ keV$, in order to detect obscured AGN beyond $z = 2$, where many SCUBA sources are being identified. The deepest current X-ray surveys however (Alexander et al. 2003), suggest that the low detection rate of X-ray emission from SCUBA sources in less deep surveys is more likely to be due to low AGN luminosity rather than heavy obscuration, which would tend to support the statement at the start of this section.

Star-formation may also be the dominant source of the far-IR bolometric luminosity of galaxies containing relatively bright X-ray emitting AGN. Certainly the significant sub-mm measurements of X-ray sources in other studies indicates that this is the case. Even a modest sub-mm flux equates to a high far-IR luminosity, whatever dust SED is assumed.

We conclude that in general the two extra-galactic backgrounds are mainly produced by different processes, with the sub-mm background being predominantly produced by dust being heated by starlight, and the X-ray background being dominated by accretion onto super-massive black-holes.

ACKNOWLEDGEMENTS

TJW wishes to thank Mat Page for his invaluable advice about the XMM data reduction, Loretta Dunne for her help with the far-IR luminosity calculations and the referee for making useful comments leading to a clearer paper. TJW acknowledges the support of a departmental postgraduate grant. SAE thanks the Leverhume Trust for a research fellowship. TXT acknowledges the partial financial support of NASA grant NAG5-9900.

REFERENCES

Alexander D. M., et al., 2003, AJ, in press (astro-ph/0211267)
Almaini O, 2000 (astro-ph/0001098)
Almaini O., Lawrence A., Boyle B. J., 1999, MNRAS, 305, L59
Almaini O. et al., 2001, MNRAS, submitted (astro-ph/0108400)
Antonucci R., 1993, ARA&A, 31, 473
Barger A. J., Cowie L. L., Sanders D. B., Fulton E., Taniguchi Y., Sato Y., Kawara K., Okuda H., 1998, Nature, 394, 248
Barger A. J., Cowie L. L., Steffen A. T., Hornschemeier A. E., Brandt W. N., Garmire G. P., 2001, ApJ, 560, L23
Barger A. J., Cowie L. L., Brandt W. N., Capak P., Garmire G. P., Hornschemeier A. E., Steffen A. T., Wehner E. H., 2002, AJ, 124, 1839
Bautz M. W., Malm M. R., Baganoff F. K., Ricker G. R., Canizares C. R., Brandt W. N., Hornschemeier A. E., Garmier G. P., 2000, ApJ, 543, L119
Brandt W. N. et al., 2001, AJ, 122, 1
Chapman S. C., Blain A. W., Ivison R. J., Smail I., 2003, Nature, in press
Dunne L., Eales S. A., 2001, MNRAS, 327, 697
Eales S. A., Lilly S., Gear W. K., Dunne L., Bond R. J., Hammer F., Le Fèvre O., Crampton D., 1999, ApJ, 515, 518
Eales S. A., Lilly S., Webb T., Dunne L., Gear W. K., Clements D., Yun M., 2000, AJ, 120, 2244
Fabian A. C. et al., 2000, MNRAS, 315, L8
Fixsen D. J., Dwek E., Mather J. C., Bennet C. L., Shafer R. A., 1998, ApJ, 508, 123
Franceschini A., Braito V., Fadda D., 2002, MNRAS, 335, L51
Gilli R., Salvati M., Hasinger G., 2001, A&A, 366, 407
Gunn K. F., Shanks T., MNRAS, submitted (astro-ph/9909089)
Hammer F., Crampton D., Lilly S., Le Fèvre O., Kenet T., 1995, MNRAS, 276, 1085
Hasinger G. et al., 2001, A&A, 365, L45
Hauser M. G. et al., 1998, ApJ, 508, 25
Hornschemeier A. E. et al., 2000, ApJ, 514, 49
Hughes D. H. et al., 1998, Nature, 394, 241
Ivison R. J. et al., 2002, MNRAS, in press (astro-ph/0206432)
Iwasawa K., Comastri A., 1998, MNRAS, 297 1219
Lilly S. J., Le Fèvre O., Crampton D., Hammer F., Tresse L., 1995, ApJ, 455, 50
Lira P., Ward M. J., Zezas A., Murray S. S., 2002, MNRAS, 2002, 333, 709
Mainieri V., Bergeron J., Rosati P., Hasinger G., Lehmann I., 2002, (astro-ph/0202211)
Miyaji T., Griffiths R. E., 2001, (astro-ph/0106028)
Nenkova M., Ivezić Ž., Elitzur M., 2002, ApJ, 570, L9
Page M. J., Stevens J. A., Mittaz J. P. D., Carrera F. J., 2001, Science, 294, 2516
Phillipps S., Davies J., 1991, MNRAS, 251, 105
Puget J. L. et al., 1996, A&A, 308, L5
Rosati P. et al., 2002, ApJ, 566, 667
Schade D., Crampton D., Hammer F., Le Fèvre O., Lilly S. J., 1996, MNRAS, 278, 95
Schmitt H. R., Kinney A. L., Calzetti D., Storchi-Bergmann T., 1997, AJ, 114, 592
Smail I., Ivison R. J., Blain A. W., 1997, ApJ, 490, 5
Valtchanov I., Pierre M., Gastaud R., 2001, A&A, 370, 689
Webb T. M., Eales. S., Lilly S. J., Clements D. L., Dunne L., Gear W. K., Flores H., Yun M., 2002, submitted (astro-ph/0201180)
Webb T. et al. in preparation